Journal of Alloys and Compounds 509 (2011) L331–L335

Contents lists available at ScienceDirect

Journal of Alloys and Compounds

journal homepage: www.elsevier.com/locate/jallcom

Letter

Resonant and non-resonant microwave absorption in the magnetoelectric $YCrO_3$ through ferro-paraelectric transition

G. Alvarez[a,*], H. Montiel[b], M.P. Cruz[c], A.C. Durán[c], R. Zamorano[a]

[a] *Sección de Estudios de Posgrado e Investigación, ESFM-IPN, U.P. Adolfo López Mateos Edificio 9, Av. Instituto Politécnico Nacional S/N, San Pedro Zacatenco, México DF 07738, Mexico*
[b] *Departamento de Tecnociencias, Centro de Ciencias Aplicadas y Desarrollo Tecnológico de la Universidad Nacional Autónoma de México, Apartado Postal 70-186, México DF 04510, Mexico*
[c] *Centro de Nanociencias y Nanotecnología, Universidad Nacional Autonoma de Mexico, Km. 107, Carretera Tijuana Ensenada, Ensenada, Baja California 22860, Mexico*

ARTICLE INFO

Article history:
Received 2 December 2010
Received in revised form 7 June 2011
Accepted 15 June 2011
Available online 21 June 2011

Keywords:
Magnetoelectric
Ferro-paraelectric transition
Electron paramagnetic resonance
Non-resonant microwave absorption

ABSTRACT

An electron paramagnetic resonance (EPR) study in the polycrystalline magnetoelectric $YCrO_3$ is carried out at X-band (8.8–9.8 GHz) in the 300–510 K temperature range. For all the temperatures, the EPR spectra show a single broad line attributable to Cr^{3+} ($S = 3/2$) ions. The onset of the ferro-paraelectric transition has been determined from the temperature dependence of three main parameters deduced from the EPR spectra: the peak-to-peak linewidth (ΔH_{pp}), the integrated intensity (I_{EPR}) and the g-factor; these parameters indicate a behavior in agreement with a diffuse phase transition. Low-field microwave absorption (LFMA) is used to give a further knowledge on this material; where this technique also gives evidence of the ferro-paraelectric transition.

1. Introduction

The term multiferroic is associated with phenomena in which at least two of the three properties ferroelectricity, ferromagnetism, and ferroelasticity occur in the same material [1,2]. In particular, the multiferroic materials in which ferroelectricity coexists with a magnetic order are called magnetoelectrics [3]; representing a kind of material in which magnetization can be induced by an electric field and electrical polarization by a magnetic field [4,5]. These materials have received much attention in recent years because of the possibility of new device applications envisaged from a strong coupling between these parameters [6]. Some magnetoelectric materials exhibit a ferroelectric transition at a relatively high temperature and a magnetic transition at lower temperature [7,8].

In particular, the orthochromites $RCrO_3$ (R = Y and rare earth) are an interesting family of compounds showing a large variety of physical and chemical properties, depending of the rare earth ion lying in the A-site of the perovskite-type structure [9]. One of these compounds is the $YCrO_3$ perovskite, which has a crystalline structure indexed as an orthorhombic cell with Pbnm space group in a large number of works [9–11]. Industrial applications of the $YCrO_3$ perovskite include its use as interconnection for the solid oxide fuel cells [12], while in pure science it has been applied to develop a model for defective structures [13]. Additionally, this compound is an antiferromagnet with a weak ferromagnetism below $T_N = 140$ K [14–17]; where the Cr^{3+} ($S = 3/2$) ion is of primary importance for the magnetic properties of this material. Also, the $YCrO_3$ perovskite is an intriguing ferroelectric material, since the existence of ferroelectricity for their centrosymmetric crystalline structure (Pbnm) [16,18]; with a Curie temperature (T_C) in the 410–450 K range [16,19]. The off-centering distortion remains a puzzle, for instance, Ramesha et al. [18] have proposed the concept of 'local non-centrosymmetry' to account for the observed permittivity peak and the small value of the polarization reported by Serrao et al. [16]; arising from 0.01 Å displacement of Cr^{3+} ions along the c axis with respect to the center of B octahedra, and which it maintains the orthorhombic symmetry for the average crystallographic structure. For the above-mentioned, the weak ferroelectric $YCrO_3$ is a representative of the split-order multiferroics, in which the ferroelectric and magnetic orders arise consecutively at low temperature.

On the other hand, the electron paramagnetic resonance (EPR) is the most powerful spectroscopic method available to unambiguously determine the valence state of paramagnetic ions [20,21], local structural information, and symmetry of paramagnetic ions incorporated in the structure [21,22]. Recently, this technique has also allowed the investigation of the ferro-paraelectric transition in magnetoelectric materials [23,24]. Additionally, we have

---

* Corresponding author.
E-mail address: memodin@yahoo.com (G. Alvarez).

0925-8388/$ – see front matter © 2011 Elsevier B.V. All rights reserved.
doi:10.1016/j.jallcom.2011.06.064

implemented a technique to measure non-resonant microwave absorption around zero magnetic field [25], which has been denominated low-field microwave absorption (LFMA). This technique has been used to detect the magnetic [17,24,26] and electric [24,27] transitions in materials, and provide a high sensitive detection of magnetic and electric orders.

To our knowledge, however, studies of the magnetoelectric $YCrO_3$ with EPR and LFMA techniques are scarce. Recently, we have published a microwave absorption study in $YCrO_3$ perovskite at low temperature [17]. In this work, the changes in the EPR lineshape are studied for a polycrystalline sample of $YCrO_3$ in the 300–510 K temperature range; these changes are quantified by means of the following parameters: the peak-to-peak linewidth (ΔH_{pp}), the integrated intensity (I_{EPR}) and the g-factor as a function of temperature, through ferro-paraelectric transition. LFMA technique is used to give a further knowledge on this material, giving also evidence of a diffuse electric transition.

2. Experimental details

Polycrystalline samples of $YCrO_3$ are prepared from stoichiometric amounts of Y_2O_3 (99.99% purity) and Cr_2O_3 (99.97% purity) by the standard solid-state reaction method. Reagents are ground and mixed to obtain a homogeneous mixture, which is followed by sintering at 1550 °C for 10 h under air atmosphere. The X-ray diffraction (XRD) of powder samples is obtained with a Philips X'Pert diffractometer using the 1.5406 Å CuKα line; XRD measurements are made at 300 K. In this investigation, we used a JEOL JES-RES 3X spectrometer operating at X-band (8.8–9.8 GHz) adequately modified [25]. For these studies, the microwave absorption response with modulation (100 kHz) on the applied dc magnetic field (H_{dc}) is measured. The microwave measurements were carried out in the 300–510 K temperature range. In EPR spectra, H_{dc} could be varied from 0 to 6000 G. During all the experiments a speck of DPPH is used as a g-marker ($g = 2.0036$) whose signal is subtracted digitally to facilitate line shape fitting. LFMA measurements are performed using a Jeol ES-ZCS2 zero-cross sweep unit that digitally compensates for any remanence in the electromagnet, allowing the measurements to be carried out by cycling H_{dc} about their zero value, continuously from −1000 to 1000 G with a standard deviation of less than 0.2 G for the measured field. In the LFMA response, the sample is zero-field heated to the desired temperature, and is then maintained at a fixed temperature with a maximum deviation of ±1 K during the entire LFMA measurement (~4 min of sweep).

3. Results and discussion

The XRD pattern of the polycrystalline sample is shown in Fig. 1. All the diffraction lines are indexed as an orthorhombic structure corresponding to space group Pnma, which are in good agreement with the literature [19,28,29]; and it shows that our material is free of secondary phases, indicating that the microwave absorption is due only to the $YCrO_3$ phase.

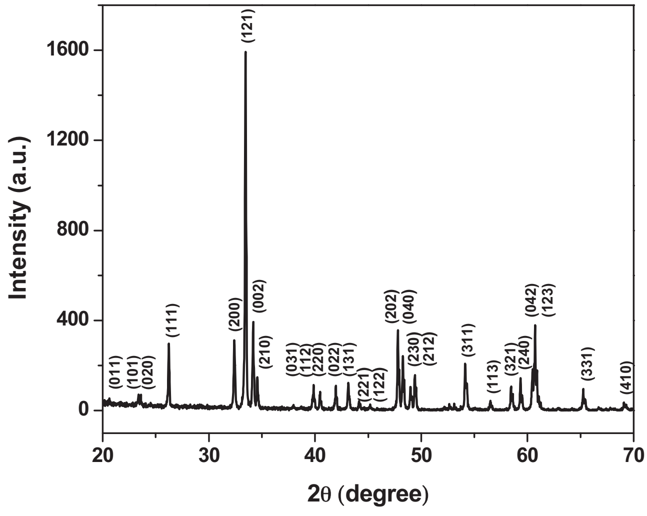

Fig. 1. XRD pattern of the polycrystalline sample of $YCrO_3$, sintering at 1550 °C for 10 h.

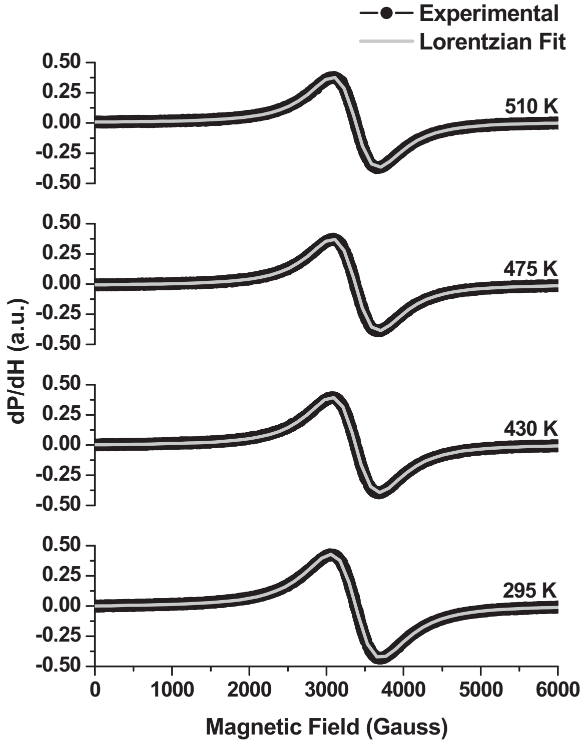

Fig. 2. EPR spectra of the magnetoelectric $YCrO_3$ for selected temperatures in the 300–510 K temperature range; the solid lines correspond to the fits obtained from Eq. (1).

In Fig. 2, we show EPR spectra (dP/dH vs. magnetic field) recorded in the 300–510 K temperature range. It can be observed that resonance spectra exhibit a single broad symmetric Lorentzian line along the entire temperature range, due to the spin of the Cr^{3+} ($S = 3/2$) ions. The derivative of microwave power absorption with respect to static field (dP/dH) is fitted into the two-component Lorentzian equation accounting for contributions from the clockwise and anticlockwise rotating components of the microwave magnetic field [30,31], as follows:

$$\frac{dP}{dH} \propto \frac{d}{dH}\left(\frac{\Delta H_{pp}}{(H_{dc}-H_{res})^2+\Delta H_{pp}^2}+\frac{\Delta H_{pp}}{(H_{dc}+H_{res})^2+\Delta H_{pp}^2}\right) \qquad (1)$$

where H_{dc} and H_{res} are the applied magnetic field and the resonant magnetic field, respectively. An extremely good fit is obtained for all the EPR spectra, as is shown in Fig. 2. The temperature dependences of the EPR parameters (ΔH_{pp}, I_{EPR}, and the g-factor) obtained from these fits are plotted in Fig. 3.

Fig. 3(a) shows the temperature dependence of the peak-to-peak linewidth (ΔH_{pp}) for $YCrO_3$ powders, which diminishes monotonically as temperature increases from 300 to 430 K. In paramagnetic materials, the microwave absorption decreases as temperature increases [21,22], and therefore the $YCrO_3$ perovskite has a behavior paramagnetic for this temperature region. As temperature increases further, $T > 430$ K, ΔH_{pp} decreases continuously but with a lower change rate. This behavior could be due to a ferro-paraelectric transition, as has been observed in other magnetoelectric materials [23,24], and that we confirmed directly by means of dielectric measurements. Fig. 4 shows the thermal variation of dielectric constant of the sample $YCrO_3$ through the ferro-paraelectric transition; where a broad peak is clearly seen at about 450 K. The dependence of the peak maxima with the frequency indicates a diffuse phase transition rather than a clas-

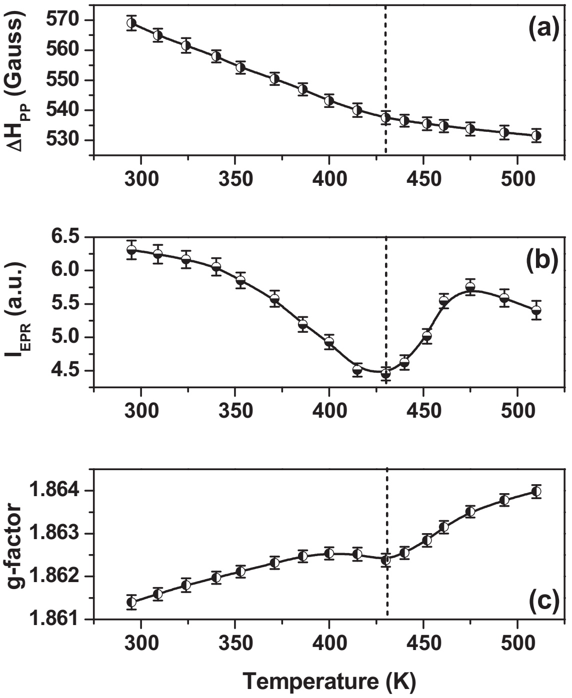

Fig. 3. Temperature dependence of (a) the peak-to-peak linewidth – ΔH_{pp}, (b) the integral intensity – I_{EPR} and (c) the g-factor in the 300–510 K temperature range. Solid lines are guides for the eye only.

sic ferro-paraelectric phase transition. Additionally, the behavior of the transition around 450 K is typical of a relaxor material where the magnitude of the dielectric constant decreases with the increase of the frequencies at the same time that the maximum is shifted to higher temperatures [32,33]. Then, we associate the ΔH_{pp} behavior to presence of a local non-centrosymmetry, that it accompanies to ferro-paraelectric transition in this material [16,18]; and which produces discreet variations in the vicinity of the Cr^{3+} ions, generating a reorganization of the spin–spin and spin–magnetic field interactions. However, more evidence is gathered below.

The temperature dependence of I_{EPR}, which in the paramagnetic phase is directly proportional to the static spin susceptibility [21,22], is shown in Fig. 3(b). Starting from room temperature, I_{EPR} decreases continuously as temperature increases, exhibiting a minimum at 430 K, followed by an increase until 475 K; and for $T > 475$ K, a slow decrease is observed. A very similar behavior was observed in the magnetoelectric $Pb(Fe_{0.5}Nb_{0.5})O_3$, and that it has been associated with a ferro-paraelectric phase transition [23]. Therefore, the minimum observed is due to onset of the dielectric transition, where the change in electrical ordering caused by the ferro-paraelectric phase transition leads to a redistribution of the electron spins; and which is in concomitance with the local character of the Cr off-centring, affecting the Cr–O–Cr angle that defines these magnetic interactions. The Curie temperature obtained by EPR technique is in a good agreement with our dielectric measurements.

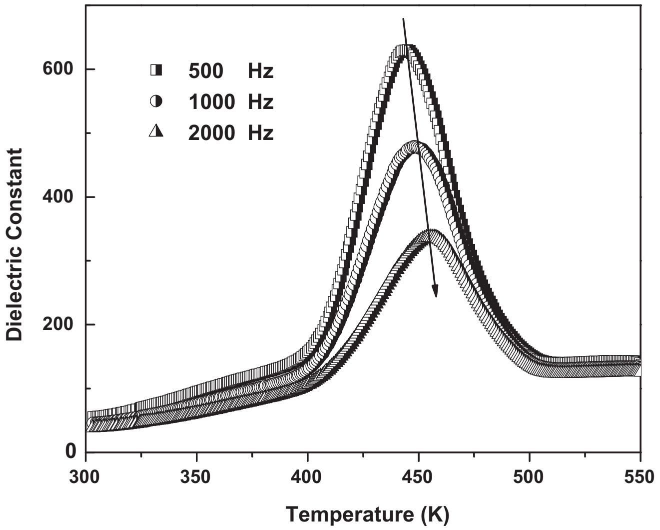

Fig. 4. Temperature variations of the dielectric constant at several frequencies for the magnetoelectric $YCrO_3$ through the ferro-paraelectric transition.

Fig. 3(c) shows the behavior of the g-factor vs. temperature, which is estimated from the resonance field (H_{res}), with $g = h\nu/\mu_B H_{res}$; where h is the Planck constant, ν is the frequency and μ_B is the Bohr magneton. Our experiments give a g-factor smaller than that of a free electron ($g = 2.0023$, $S = 1/2$), along the entire temperature range. For a powder sample is expected that the internal field affects are average, and we believe that the observed variation of the g-factor with temperature is intrinsic to sample. Additionally, this behavior can be explained through the spin value of Cr^{3+} ($S = 3/2$) ions and to changes in the spin–orbit coupling. The effective g-factor (g_{eff}) of a paramagnetic center is given by $g_{eff} = g(1 \pm \kappa/\Delta)$, where Δ is the crystal-field splitting and κ is the spin–orbit coupling constant. A gradual decrease of the orbital ordering takes place when the temperature is increased from 300 to 400 K, originating a change in the spin–orbit coupling as well as in the crystal-field splitting, and which can give rise to the observed increase in the g-factor for this temperature range. As the temperature increases further, the g-factor decreases, with a local minimum at 430 K ($g_{min} = 1.8624$); we associate this feature with the onset of the ferro-paraelectric phase transition. The additional g-factor increase (from 430 K to 510 K; $g = 1.8640$) is associated with the paramagnetic behavior of the Cr ions [23]. Additionally, in Fig. 3(c), we can establish two behavior regions that are limited to 430 K, and that they can be associated with the diffuse character of the ferro-paraelectric transition [16,19]; which is detected starting from 400 K.

We turn now to the LFMA results. Fig. 5(a) shows LFMA spectra (dP/dH vs. magnetic field, around zero field) for selected temperatures. The curves exhibit a linear behavior with a positive slope and non-hysteretic traces. The positive slope implies that this non-resonant microwave absorption is a minimum around zero magnetic field, and that it increases with applied magnetic field; in other words, this is a magnetic field-dependent absorption. LFMA lines show the absence of any irreversible microwave energy-absorption process in the ordered and disordered electric phases. This behavior contrasts strongly with the one shown by other materials [26,34].

The LFMA line can be described by the experimental correlation:

$$\frac{dP}{dH} = S(T)H \tag{2}$$

where $S(T)$ is the slope of the absorption line and that it depends only on temperature.

Fig. 5(b) shows the behavior of the slope of the LFMA line obtained of the fits for the 300–510 K temperature range. Starting from room temperature, as the temperature increased, the slope decreases monotonically; reaching a minimum value at $T_{min} = 430$ K. This decreasing behavior is characteristic of a paramagnetic phase [27], in a good agreement with the EPR results. After T_{min}, when the temperature continues to increase, the slope increases until 475 K; for $T > 475$ K a slow decrease in slope is

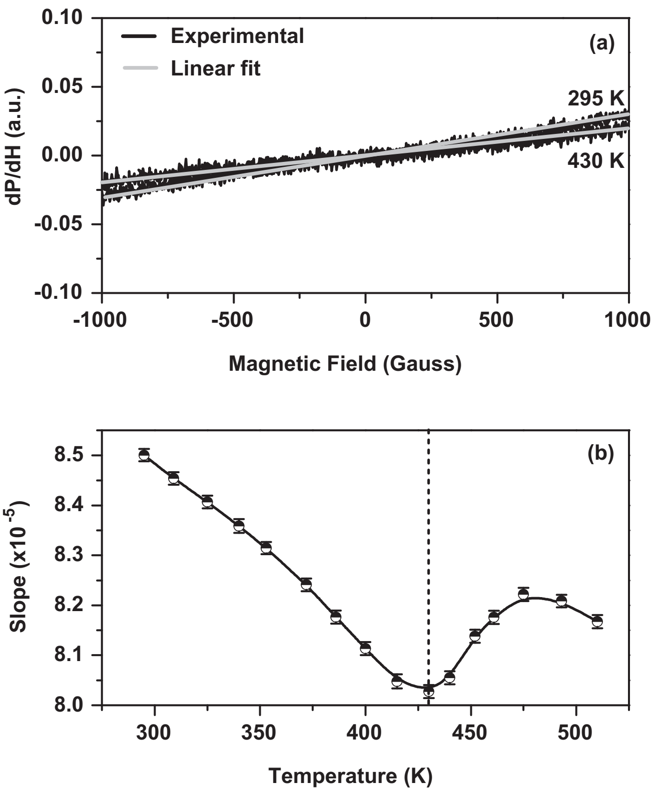

Fig. 5. (a) LFMA spectra for 295 K and 430 K, with $H_{\mathrm{mod}} = 0.63$ G and microwave power of 1 mW; the solid lines correspond to the fits obtained from Eq. (2). (b) The temperature dependence of the absorption line slope for temperature interval of 300–510 K; the curves connecting points are only guides for the eye.

observed. A very similar behavior has been previously observed in other magnetoelectric material [27]. We associate the minimum (T_{min}) of this profile with the onset of the ferro-paraelectric transition, as it is suggested by dielectric measurements of the Fig. 4; and which is accompanied for a local non-centrosymmetry [18]. Where it leads to a discreet redistribution of the Cr^{3+} ions, originating a change in the relative orientation of magnetic moments; and it affects the superexchange interactions between Cr ions, generating a change in the microwave absorption dynamics.

On the other hand, it is necessary to mention that the microwave absorption is related with the imaginary part of the magnetic permeability [35]. As the material under study is a dielectric, the only current which can flow is the Maxwell displacement current (E_{in}). Since the sample, in the resonant cavity, is located in the place of maximum ac magnetic field [25,27], the microwave absorption must decrease when the dielectric permittivity (ε) increases to satisfy the boundary conditions ($D_{\mathrm{normal}} = \varepsilon E_{\mathrm{in}}$ and $E_{\mathrm{out}} = D_{\mathrm{out}} \sim 0$; where D is the displacement). The plot of dielectric constant vs. temperature to several rf frequencies is illustrated in the Fig. 4, where the dielectric constant shows a maximum at the temperature of Curie. Therefore, the maximum in dielectric constant should coincide with the minimum of the microwave absorption close to the ferro-paraelectric transition. The Curie temperature ($T_{\mathrm{min}} = 430$ K) obtained by the technique LFMA is in a good agreement with our dielectric measurements. The whole profile of the slope of the LFMA line depends on the thermal dependence of the absorption dynamics of the paramagnetic moments around ferro-paraelectric transition.

Additionally, the microwave absorption dynamics shows characteristic of a diffuse phase transition, i.e., the transition region is extended throughout a wide temperature range. This characteristic can be ascribed to that the relaxor materials are highly inhomogeneous materials in which a diffuse transition is due to a multitude of local phase transitions with different Curie temperatures in a broad range of temperature [36], as it is shown in $\mathrm{YCrO_3}$.

4. Conclusions

The changes in the parameters ΔH_{pp}, I_{EPR} and g-factor in the EPR spectra for the magnetoelectric $\mathrm{YCrO_3}$ at $T_{\mathrm{min}} = 430$ K, are interpreted as a diffuse ferro-paraelectric transition. This transition, that is associated with a local non-centrosymmetry, promotes a spin redistribution of Cr^{3+} ions, which creates changes in dynamics of microwave absorption in the magnetoelectric $\mathrm{YCrO_3}$. For all temperatures, LFMA spectra showed straight lines with positive slope and non-hysteretic traces. The spectral changes for the plot of the slope vs. temperature give also evidence of a ferro-paraelectric transition and also suggest a diffuse character, with a very high detection sensibility.

Acknowledgements

G. Alvarez acknowledges a fellowship from CONACyT-Mexico (Retention Program). Support from project IPN-SIP-20110979 is gratefully acknowledged.

References

[1] K.F. Wang, J.M. Liu, Z.F. Ren, Adv. Phys. 58 (2009) 321.
[2] C.W. Nan, M.I. Bichurin, S. Dong, D. Viehland, G. Srinivasan, J. Appl. Phys. 103 (2008) 031101.
[3] D. Khomskii, Physics 2 (2009) 20.
[4] I.E. Chupis, Low Temp. Phys. 36 (2010) 477.
[5] T.H. Wang, C.S. Tu, H.Y. Chen, Y. Ding, T.C. Lin, Y.D. Yao, V.H. Schmidt, K.T. Wu, J. Appl. Phys. 109 (2011) 044101.
[6] G. Srinivasan, Annu. Rev. Mater. Res. 40 (2010) 153.
[7] N. Hur, I.K. Jeong, M.F. Hundley, S.B. Kim, S.W. Cheong, Phys. Rev. B 79 (2009) 134120.
[8] Y. Du, Z.X. Cheng, X.L. Wang, P. Liu, S.X. Dou, J. Appl. Phys. 109 (2011) 07B507.
[9] J.B. Goodenough, W. Gräper, F. Holtzberg, D.H. Huber, R.A. Lefever, J.M. Longo, T.R. McGuire, S. Methfessel, Landolt-Börnstein-Band 4: Magnetische And Andere Eigenschaften Von Oxide Und Verwandten Verbindungen, Springer-Verlag, Berlin, Heidelberg, New York, 1970.
[10] S. Geller, E.A. Good, Acta Crystallogr. 1 (1967) 948.
[11] S. Quezel-Ambrunaz, M. Mareschal, Bull. Soc. Fr. Miner. Crystallogr. 86 (1963) 204.
[12] S. Wang, B. Lin, Y. Dong, D. Fang, H. Ding, X. Liu, G. Meng, J. Power Sources 188 (2009) 483.
[13] G. Carini II., H. Anderson, M. Nasrallah, D. Sparlin, J. Solid State Chem. 94 (1991) 329.
[14] V.M. Judin, A.B. Sherman, Solid State Commun. 4 (1966) 661.
[15] T. Morishita, K. Tsushima, Phys. Rev. B 24 (1981) 341.
[16] C.R. Serrao, A.K. Kundu, S.B. Krupanidhi, U.V. Waghmare, C.N.R. Rao, Phys. Rev. B 72 (2005) 220101.
[17] G. Alvarez, M.P. Cruz, A.C. Durán, H. Montiel, R. Zamorano, Solid State Commun. 150 (2010) 1597.
[18] K. Ramesha, A. Llobet, T. Proffen, C.R. Serrao, C.N.R. Rao, J. Phys.: Condens. Matter 19 (2007) 102202.
[19] A. Durán, A.M. Arévalo-López, E. Castillo-Martínez, M. García-Guaderrama, E. Moran, M.P. Cruz, F. Fernández, M.A. Alario-Franco, J. Solid State Chem. 183 (2010) 1863.
[20] D. Ramírez-Rosales, R. Zamorano-Ulloa, O. Pérez-Martinez, Solid State Commun. 118 (2001) 371.
[21] G. Alvarez, in: Herlinda Montiel, Guillermo Alvarez (Eds.), Advances in Non-crystalline Solids: Metallic Glass Formation, Magnetic Properties and Amorphous Carbon Films, Transworld Research Network, Kerala, India, 2010.
[22] J.A. Weil, J.R. Bolton, J.E. Wertz, Electron Spin Resonance: Elementary Theory and Practical Applications, John Wiley & Sons Inc., New York, 1994.
[23] G. Alvarez, R. Font, J. Portelles, R. Valenzuela, Mater. Lett. 62 (2008) 1737.
[24] G. Alvarez, H. Montiel, J.A. Peña, M.A. Castellanos, R. Zamorano, J. Alloys Compd. 508 (2010) 471.
[25] G. Alvarez, R. Zamorano, J. Alloys Compd. 369 (2004) 231.
[26] V.P. Nabereznykh, M.I. Tsindlekht, JETP Lett. 36 (1982) 157.
[27] G. Alvarez, R. Font, J. Portelles, R. Zamorano, R. Valenzuela, J. Phys. Chem. Solids 68 (2007) 1436.
[28] T. Tachiwaki, Y. Kunifusa, M. Yoshinaka, K. Hirota, O. Yamaguchi, Int. J. Inorg. Mater. 3 (2001) 107.

[29] V. Bedekar, R. Shukla, A.K. Tyagi, Nanotechnology 18 (2007) 155706.
[30] V.A. Ivanshin, J. Deisenhofer, H.A. Krug von Nidda, A. Loidl, A. Mukhin, J. Balbashov, M.V. Eremin, Phys. Rev. B 61 (2000) 6213.
[31] J.P. Joshi, R. Gupta, A.K. Sood, S.V. Bhat, A.R. Raju, C.N.R. Rao, Phys. Rev. B 65 (2002) 024410.
[32] C. Randall, A. Bhalla, T. Shrout, L.E. Cross, J. Mater. Res. 5 (1990) 829.
[33] L.E. Cross, Ferroelectrics 76 (1987) 241.
[34] G. Alvarez, H. Montiel, J.F. Barron, M.P. Gutierrez, R. Zamorano, J. Magn. Magn. Mater. 322 (2010) 348.
[35] C.A. Balanis, Advanced Engineering Electromagnetics, first ed., John Wiley & Sons, USA, 1989.
[36] D. Viehland, S.J. Jang, L.E. Cross, J. Appl. Phys. 68 (1990) 2916.